Structural Engineering and Mechanics, *Vol. 66, No. 1 (2018) 113-124*
DOI: https://doi.org/10.12989/sem.2018.66.1.113

Reflection and refraction of plane waves in layered nonlocal elastic and anisotropic thermoelastic medium

Parveen Lata*

Department of Basic and Applied Sciences, Punjabi University, Patiala, Punjab, India

(Received January 24, 2018, Revised February 18, 2018, Accepted February 19, 2018)

Abstract. In the present paper, we have considered a layered medium of two semi-infinite nonlocal elastic solids with intermediate transversely isotropic magnetothermoelastic solid. The intermediate slab is of uniform thickness with the effects of two temperature, rotation and Hall current and with and without energy dissipation. A plane longitudinal or transverse wave propagating through one of the nonlocal elastic solid half spaces, is made incident upon transversely isotropic slab and it results into various reflected and refracted waves. The amplitude ratios of various reflected and refracted waves are obtained by using appropriate boundary conditions. The effect of nonlocal parameter on the variation of various amplitude ratios with angle of incidence are depicted graphically. Some cases of interest are also deduced.

Keywords: interface; reflection; transmission; transversely isotropic thermoelastic; nonlocal elastic half space; amplitude ratios

1. Introduction

The nonlocal theory of continuum mechanics is of recent origin. It takes into account the fact that the interacting forces between material points are far reaching in character. From the systematic point of view, it differs from the classical theory by assuming the balance laws to be valid only on the whole of the body. In some cases, such as in phonon dispersion in solids, in electromagnetic solids, when the continuity hypothesis made in classical theory can no longer be supported because of the discrete characteristics of the medium, only a non-local theory might provide the right answer while the classical one would fail. Many researchers developed the theory of nonlocal elasticity year to year e.g., (Kroner 1967, Edelen and Law 1971, Eringen and Edelen 1972, Polizzotto 2001, Vasilev and Lurie 2016, Singh *et al*. 2017).

Layered structures are widely used in diverse applications such as spacecraft, aircraft, automobiles, boats and ships due to their substantial bending strength and impact resistance at a light weight. The dynamic applications have motivated various studies of wave propagation and dynamic flexural deformation of multilayer beams and plates. Elphinstone and Lakhtakia (1994) have investigated the response of a plane wave incident on a chiral solid slab sandwiched between two elastic half spaces. Khurana and Tomar (2009) discussed longitudinal wave response of chiral slab interposed between micropolar elastic solid half spaces. Wave propagation in layered medium has been investigated by many researchers (Chaudhary *et al*. 2010, Deshpande and Fleck 2005, Liu and Bhattacharya 2009, Marin and Baleanu 2016).

As the importance of anisotropic devices has increased in many fields of optics and microwaves, wave propagation in anisotropic media has been widely studied over in the last decades. Mathematical modeling of plane wave propagation along with the free boundary of an elastic half-space has been subject of continued interest for many years. Keith and Crampin (1977) derived a formulation for calculating the energy division among waves generated by plane waves incident on a boundary of anisotropic media. Reflection of plane waves at the free surface of a transversely isotropic thermoelastic diffusive solid half-space has been discussed by (Kumar and Mukhopadhyay 2010, Othman 2010, Kumar and Kansal 2011, Kaushal *et al*. (2011), Said and Othman 2016). Wave propagation has remained the study of concern of many researchers (Marin 1997, Marin 2008, Marin 2016, Kumar and Gupta 2013, Kumar *et al*. 2016a, 2016b, Othman and Abd-elaziz 2017).

Chen and Gurtin (1968), Chen *et al.* (1968) and Chen *et al.* (1969) have formulated a theory of heat conduction in deformable bodies which depends upon two distinct temperatures, the conductive temperature φ and the thermo dynamical temperature T. For time independent situations, the difference between these two temperatures is proportional to the heat supply, and in absence of heat supply, the two temperatures are identical. For time dependent problems, the two temperatures are different, regardless of the presence of heat supply. The two temperatures T, φ and the strain are found to have representations in the form of a travelling wave plus a response, which occurs instantaneously throughout the body (Boley and Tolins 1962). The wave propagation in two temperature theory of thermoelasticity was investigated by Warren and Chen (1973).

Green and Naghdi (1991, 1992, 1993) postulated a new

*Corresponding author, Ph.D.
E-mail: parveenlata@pbi.ac.in

http://www.techno-press.com/journals/sem&subpage=7
ISSN: 1225-4568 (Print), 1598-6217 (Online)

concept in thermoelasticity theories and proposed three models which are subsequently referred to as GN-I, II, and III models. A comprehensive work has been done in thermoelasticity theory with and without energy dissipation and thermoelasticity with two temperatures (Youssef 2011, Youssef 2006, Sharma and Marin 2013, Sharma and Bhargav 2014, Kumar *et al.* 2016).

In view of the fact that most of the large bodies like the earth, the moon and other planets have an angular velocity, as well as earth itself behaves like a huge magnet, it is important to study the propagation of thermoelastic waves in a rotating medium under the influence of magnetic field. So, the attempts are being made to study the propagation of finite thermoelastic waves in an infinite elastic medium rotating with angular velocity. Several authors (Das and Kanoria 2014, Jahangir 2012, Atwa and Jahangir 2014, Othman and Jahangir 2015, Ezzat and Bary 2016, Ezzat and Bary 2017) have studied various problems in generalized thermoelasticity to study the effect of rotation.

Here in this paper, we consider transversely isotropic magnetothermoelastic solid slab of uniform thickness, interposed between two different semi-infinite homogeneous isotropic nonlocal elastic solids. A plane longitudinal or transverse wave propagating through one of the nonlocal elastic solid half spaces, is made incident upon transversely isotropic magnetothermoelastic solid. We have presented the reflection and transmission coefficients obtained separately, corresponding to the appropriate set of boundary conditions. The variations in the modulus of the amplitude ratios with the angle of incidence are depicted graphically.

2. Basic equations

Following Achenbach (1973) and Eringen (1972), the equations of motion for the nonlocal elastic half space are

$$\mu^l u^l_{i,jj} + (\lambda^l + \mu^l)u^l_{i,ij} = \rho^e(1-\varepsilon^2\nabla^2)\frac{\partial^2 \boldsymbol{u}_i{}^l}{\partial t^2}\ , \quad (i,j = 1,2,3\ and\ l = 1,2) \tag{1}$$

and the constitutive relations are

$$t_{ij,j}{}^l = 2\mu^l u^l_{i,j} + \lambda^l u^l_{k,k}\delta_{ij}\ , \quad (i,j,k = 1,2,3\ and\ l = 1,2) \tag{2}$$

Following Lata *et al.* (2016), equation of motion for a transversely isotropic thermoelastic medium rotating uniformly with an angular velocity $\boldsymbol{\Omega} = \Omega n$, where n is a unit vector representing the direction of axis of rotation and taking into account Lorentz force

$$t_{ij,j} + F_i\ =\ \rho\{\ddot{u}_i + \big(\boldsymbol{\Omega}\times(\boldsymbol{\Omega}\times u)\big)_i + (2\boldsymbol{\Omega}\times\dot{u})_i\ \}, \tag{3}$$

Following Chandrasekharaia (1998) and Youssef (2006), the heat conduction equation with two temperature and with and without energy dissipation is given by

$$K_{ij}\varphi_{,ij} + K^*_{ij}\dot{\varphi}_{,ij} = \beta_{ij}T_0\ddot{e_{ij}} + \rho C_E\ddot{T}\ , \tag{3}$$

and the constitutive relations for a transversely isotropic thermoelastic medium are given by

$$t_{ij} = C_{ijkl}e_{kl} - \beta_{ij}T, \tag{5}$$

Here

$F_i = \mu_0(\boldsymbol{J}\times\boldsymbol{H}_0)_i$ are the components of Lorentz force, where

$$\boldsymbol{J} = \frac{\sigma_0}{1+m^2}\left(\boldsymbol{E} + \mu_0\left(\ \dot{\boldsymbol{u}}\times\boldsymbol{H} - \frac{1}{en_e}\boldsymbol{J}\times\boldsymbol{H}_0\right)\right)\ ,\quad e_{ij} = \frac{1}{2}\big(u_{i,j}+u_{j,i}\big)\ ,\ \ i,j = 1,2,3\ ,$$

$$\beta_{ij} = C_{ijkl}\alpha_{ij}\ \text{and}\ T = \varphi - a_{ij}\varphi_{,ij},$$

$\beta_{ij} = \beta_i\delta_{ij}\,,\ K_{ij} = K_i\delta_{ij}\ ,\ K_{ij}{}^* = K_i{}^*\delta_{ij}\ ,\ i$ is not summed,

$C_{ijkl}(C_{ijkl} = C_{klij} = C_{jikl} = C_{ijlk})$ are elastic parameters, β_{ij} is the thermal tensor, T is the temperature, T_0 is the reference temperature, t_{ij} are the components of stress tensor, e_{kl} are the components of strain tensor, u_i are the displacement components, ρ is the density, C_E is the specific heat, K_{ij} is the thermal conductivity, K^*_{IJ} is the materialistic constant, a_{ij} are the two temperature parameters, α_{ij} is the coefficient of linear thermal expansion, Ω is the angular velocity of the solid, H is the magnetic strength, $\dot{\boldsymbol{u}}$ is the velocity vector , **E** is the intensity vector of the electric field, $\boldsymbol{J}$ **is** the current density vector, $m(=\omega_e t_e = \frac{\sigma_0\mu_0 H_0}{en_e})$ is the Hall parameter, t_e is the electron collision time, $\omega_e = \frac{e\mu_0 H_0}{m_e}$ is the electronic frequency, e is the charge of an electron, m_e is the mass of the electron, $\sigma_0 = \frac{e^2 t_e n_e}{m_e}$, is the electrical conductivity and n_e is the number of density of electrons. $\varepsilon = e_0 a$ is a nonlocal parameter, e_0 is a material constant and a being the internal characteristic length. The internal characteristic length a is the interatomic distance or lattice distance. λ^l, μ^l , ρ^l are the Lame's constants and density in the elastic half space. $\boldsymbol{u}_i{}^l$ $((i = 1,2,3\ and\ l = 1,2)$ are the components of displacement vector, $t_{ij,j}{}^l$ are the components of stress in elastic half space.

3. Formulation of the problem

Consider a layered model consisting of two nonlocal elastic solids with intermediate transversely isotropic magnetothermoelastic solid. The intermediate slab is of finite thickness H, with an angular velocity $\boldsymbol{\Omega}$ initially at uniform temperature T_0 with Hall current effect. Introducing the Cartesian co-ordinate system (x_1, x_2, x_3) such that x_1 −and x_3 −axis are on horizontal plane and $x_3 -$ axis is pointing vertically downwards. Let the intermediate layer occupying the region $M[0 \le x_3 \le H]$ be drawn by the planes $x_3 = 0$ and $x_3 = H$ .The two nonlocal elastic half spaces be occupying the regions : $M^{(1)}$: $[x_3 < 0]$ and $M^{(2)}$: $[x_3 > H]$. For two-dimensional problem, the displacement vectors $\boldsymbol{u}, \boldsymbol{u}^l$ $(\ l = 1,2)$ in transversely isotropic magnetothermoelastic and in nonlocal elastic half space are taken as

$$\boldsymbol{u} = (u_1, 0, u_3)\ \text{and}\ \boldsymbol{u}^l = (u^l_1, 0, u^l_3)\ ,, (l = 1,2) \tag{6}$$

We also assume that

$$\boldsymbol{E}=0,\ \boldsymbol{\Omega} = (0, \Omega, 0) \tag{7}$$

Following Slaughter (2002), using appropriate transformations, on the set of Eqs. (3) and (5) and with the aid of (6)-(7), the field equations for transversely isotropic magnetothermoelastic medium are

$$\begin{aligned} c_{11}\frac{\partial^2 u_1}{\partial x^2} + c_{13}\frac{\partial^2 u_3}{\partial x_1 \partial x_3} + c_{44}\left(\frac{\partial^2 u_1}{\partial {x_3}^2} + \frac{\partial^2 u_3}{\partial x_1 \partial x_3}\right) \\ - \beta_1 \frac{\partial}{\partial x_1}\Bigg\{\varphi \\ - \left(a_1 \frac{\partial^2 \varphi}{\partial {x_1}^2} + a_3 \frac{\partial^2 \varphi}{\partial {x_3}^2}\right)\Bigg\} - \mu_0 J_3 H_0 \\ = \rho\left(\frac{\partial^2 u_1}{\partial t^2} - \Omega^2 u_1 + 2\Omega\frac{\partial u_3}{\partial t}\right), \end{aligned} \tag{8}$$

$$\begin{aligned} (c_{13} + c_{44})\frac{\partial^2 u_1}{\partial x_1 \partial x_3} + c_{44}\frac{\partial^2 u_3}{\partial {x_1}^2} + c_{33}\frac{\partial^2 u_3}{\partial {x_3}^2} \\ - \beta_3 \frac{\partial}{\partial x_3}\Bigg\{\varphi \\ - \left(a_1 \frac{\partial^2 \varphi}{\partial {x_1}^2} + a_3 \frac{\partial^2 \varphi}{\partial {x_3}^2}\right)\Bigg\} + \mu_0 J_1 H_0 \\ = \rho\left(\frac{\partial^2 u_3}{\partial t^2} - \Omega^2 u_3 - 2\Omega\frac{\partial u_1}{\partial t}\right), \end{aligned} \tag{9}$$

$$\begin{aligned} \left(k_1 + {k_1}^*\frac{\partial}{\partial t}\right)\frac{\partial^2 \varphi}{\partial {x_1}^2} + \left(k_3 + {k_3}^*\frac{\partial}{\partial t}\right)\frac{\partial^2 \varphi}{\partial {x_3}^2} \\ = T_0 \frac{\partial^2}{\partial t^2}\left\{\beta_1 \frac{\partial u_1}{\partial x_1} + \beta_3 \frac{\partial u_3}{\partial x_3}\right\} + \rho C_E \ddot{T}. \end{aligned} \tag{10}$$

and the stress components are

$$t_{33} = c_{13}e_{11} + c_{33}e_{33} - \beta_3 T, \tag{11}$$

$$t_{13} = 2c_{44}e_{13}, \tag{12}$$

where J_1 , J_2 and J_3 are given as $J_1 = \frac{\sigma_0 \mu_0 H_0}{1+m^2}\left(m\frac{\partial u_1}{\partial t} - \frac{\partial u_3}{\partial t}\right)$, $J_2 = 0$, $J_3 = \frac{\sigma_0 \mu_0 H_0}{1+m^2}\left(\frac{\partial u_1}{\partial t} + m\frac{\partial u_3}{\partial t}\right)$, $T = \varphi - \left(a_1 \frac{\partial^2 \varphi}{\partial x_1^2} + a_3 \frac{\partial^2 \varphi}{\partial x_3^2}\right)$, $\beta_1 = (c_{11}+c_{12})\alpha_1 + c_{13}\alpha_3$, $\beta_3 = 2c_{13}\alpha_1 + c_{33}\alpha_3$.

In the above equations we use the contracting subscript notations ($11 \to 1, 22 \to 2, 33 \to 3, 23 \to 4, 31 \to 5, 12 \to 6$) to relate c_{ijkl} to c_{mn}

From Eq. (1), the field equations for the nonlocal elastic half spaces in component form are

$$\mu^l\left(\frac{\partial^2 u_1^l}{\partial {x_1}^2} + \frac{\partial^2 u_1^l}{\partial {x_3}^2}\right) + (\lambda^l + \mu^l)\frac{\partial^2 u_3^l}{\partial x_1 \partial x_3} = \rho^l(1 - \varepsilon^2\nabla^2)\frac{\partial^2 {u_1}^l}{\partial t^2}, \qquad (l = 1,2) \tag{13}$$

$$\mu^l\left(\frac{\partial^2 u_3^l}{\partial {x_1}^2} + \frac{\partial^2 u_3^l}{\partial {x_3}^2}\right) + (\lambda^l + \mu^l)\frac{\partial^2 u_1^l}{\partial x_1 \partial x_3} = \rho^l(1 - \varepsilon^2\nabla^2)\frac{\partial^2 {u_3}^l}{\partial t^2}. \qquad (l = 1,2) \tag{14}$$

The stress components for elastic half spaces in the $x_1 - x_3$ plane are

$$t_{13}^l = \mu^l\left(\frac{\partial {u_1}^l}{\partial x_3} + \frac{\partial {u_3}^l}{\partial x_1}\right) \quad , (l = 1,2) \tag{15}$$

$$t_{33}^l = (\lambda^l)\frac{\partial {u_1}^l}{\partial x_1} + (\lambda^l + 2\mu^l)\frac{\partial {u_3}^l}{\partial x_3}. \quad (l = 1,2) \tag{16}$$

To facilitate the solution, we introduce the dimensionless quantities

$$\begin{aligned} &{x_1}' = \frac{x_1}{L},\ {x_3}' = \frac{x_3}{L},\ ({u_1}', u_3', {u_1}'^l, {u_3}'^l) = \frac{\rho c_1^2}{L\beta_1 T_0}(u_1, u_3, {u_1}^l, {u_3}^l),\ T' = \frac{T}{T_0},\ t' = \frac{c_1}{L}t,\ t_{11}' = \\ &\frac{t_{11}}{\beta_1 T_0},\ J' = \frac{\rho c_1^2}{\beta_1 T_0}J (t_{33}', t_{31}', t_{13}'^l, t_{33}'^l) = \left(\frac{t_{33}}{\beta_1 T_0}, \frac{t_{31}}{\beta_1 T_0}, \frac{t_{13}^l}{\beta_1 T_0}, \frac{t_{33}^l}{\beta_1 T_0}\right),\ \varphi' = \frac{\varphi}{T_0},\ a_1' = \frac{a_1}{L},\ a_3' = \frac{a_3}{L},\ h' = \\ &\frac{h}{H_0}\ M = \frac{\sigma_0 \mu_0 H_0}{\rho c_1 L}, \Omega' = \frac{L}{c_1}\Omega \quad \text{where} \quad c_{11} = \rho c_1^2 \end{aligned} \tag{17}$$

Using dimensionless quantities defined by (17) in the Eqs. (8)-(10) and (13)-(14), and suppressing the primes, the resulting equations yield

$$\begin{aligned} \frac{\partial^2 u_1}{\partial {x_1}^2} + \delta_4\frac{\partial^2 u_3}{\partial x_1 \partial x_3} + \delta_2\left(\frac{\partial^2 u_1}{\partial {x_3}^2} + \frac{\partial^2 u_3}{\partial x_1 \partial x_3}\right) \\ - \frac{\partial}{\partial x_1}\left\{\varphi - \left(\frac{a_1}{L}\frac{\partial^2 \varphi}{\partial {x_1}^2} + \frac{a_3}{L}\frac{\partial^2 \varphi}{\partial {x_3}^2}\right)\right\} \\ - \frac{M}{1+m^2}\mu_0 H_0\left(\frac{\partial u_1}{\partial t} + m\frac{\partial u_3}{\partial t}\right) \\ = \frac{\partial^2 u_1}{\partial t^2} - \Omega^2 u_1 + 2\Omega\frac{\partial u_3}{\partial t} \end{aligned} \tag{18}$$

$$\begin{aligned} \delta_1\frac{\partial^2 u_1}{\partial x_1 \partial x_3} + \delta_2\frac{\partial^2 u_3}{\partial {x_1}^2} + \delta_3\frac{\partial^2 u_3}{\partial {x_3}^2} \\ - \frac{\beta_3}{\beta_1}\frac{\partial}{\partial x_3}\Bigg\{\varphi \\ - \left(\frac{a_1}{L}\frac{\partial^2 \varphi}{\partial {x_1}^2} + \frac{a_3}{L}\frac{\partial^2 \varphi}{\partial {x_3}^2}\right)\Bigg\} \\ + \frac{M}{1+m^2}\mu_0 H_0\left(m\frac{\partial u_1}{\partial t} - \frac{\partial u_3}{\partial t}\right) \\ = \frac{\partial^2 u_3}{\partial t^2} - \Omega^2 u_3 - 2\Omega\frac{\partial u_1}{\partial t}, \end{aligned} \tag{19}$$

$$\begin{aligned} \varepsilon_1\left(1 + \frac{\varepsilon_3}{\varepsilon_1}\frac{\partial}{\partial t}\right)\frac{\partial^2 \varphi}{\partial {x_1}^2} + \varepsilon_2\left(1 + \frac{\varepsilon_4}{\varepsilon_2}\frac{\partial}{\partial t}\right)\frac{\partial^2 \varphi}{\partial {x_3}^2} \\ = {\varepsilon_5}'{\beta_1}^2\frac{\partial^2}{\partial t^2}\left(\frac{\partial u_1}{\partial x_1} + \frac{\beta_3}{\beta_1}\frac{\partial u_3}{\partial x_3}\right) \\ + \frac{\partial^2}{\partial t^2}\left(\left\{\varphi - \frac{a_1}{L}\frac{\partial^2 \varphi}{\partial {x_1}^2} + \frac{a_3}{L}\frac{\partial^2 \varphi}{\partial {x_3}^2}\right\}\right) \end{aligned} \tag{20}$$

$\delta_1 = \frac{(c_{13}+c_{44})}{c_{11}}$, $\delta_2 = \frac{c_{44}}{c_{11}}$, $\delta_3 = \frac{c_{33}}{c_{11}}$, $\delta_4 = \frac{c_{13}}{c_{11}}$, $\varepsilon_1 = \frac{k_1}{\rho C_E c_1^2}$, $\varepsilon_2 = \frac{k_3}{\rho C_E c_1^2}$, $\varepsilon_3 = \frac{{k_1}^*}{L\rho C_E c_1}$,

$\varepsilon_4 = \frac{k_3{}^*}{L\rho C_E c_1}$, $\varepsilon_5{}' = \frac{T_0}{\rho^2 C_E c_1^2}$.

For the mediums $M^{(1)}$ and $M^{(2)}$, we have

$$\nabla^2 \phi^l = \frac{1}{(\alpha'^{(l)})^2}\left(\frac{\partial^2 \varphi^l}{\partial t^2}\right) \tag{21}$$

$$\nabla^2 \psi^l = \frac{1}{\beta'^{(l)2}}\left(\frac{\partial^2 \psi^l}{\partial t^2}\right). \tag{22}$$

where

$\alpha'^{(l)} = \frac{\alpha^{(l)}}{c_1}$, $\beta'^{(l)} = \frac{\beta^{(l)}}{c_1}$, $\alpha^{(l)} = \sqrt{\frac{(\lambda^l + 2\mu^l + +\varepsilon^2 s^2)}{\rho^l}}$ and $\beta^{(l)} = \sqrt{\frac{\mu^l + \varepsilon^2 s^2}{\rho^l}}$ are velocities of longitudinal and transverse waves respectively for the mediums $M^{(1)}$ and $M^{(2)}$ for $(l = 1{,}2)$ and ϕ^l and ψ^l are the scalar potentials defined by

$$u_1^l = \frac{\partial \phi^l}{\partial x_1} - \frac{\partial \psi^l}{\partial x_3},\quad u_3^l = \frac{\partial \phi^l}{\partial x_3} + \frac{\partial \psi^l}{\partial x_1} . \tag{23}$$

We seek a wave solution of the form for transversely isotropic magnetothermoelastic solid as

$$\begin{pmatrix} u_1 \\ u_3 \\ \varphi \end{pmatrix} = \begin{pmatrix} U_1 \\ U_3 \\ \varphi^* \end{pmatrix} \exp\{(ik(x_1 sin\theta + x_3 cos\theta) - i\omega t)\}, \tag{24}$$

where $(sin\theta, cos\theta)$ denotes the projection of the wave normal onto the $x_1 - x_3$ plane, k and ω are respectively the wave number and angular frequency of plane waves propagating in $x_1 - x_3$ plane.

Upon using (24) in (18)-(20) and then eliminating U_1, U_3 *and* φ^* from the resulting equations yields the following characteristic equation

$$Ak^6 + Bk^4 + Ck^2 + D = 0. \tag{25}$$

where A, B, C, D are given in appendix A.

The roots of Eq. (25) gives six values of k , in which we are interested to those roots whose imaginary parts are positive. Corresponding to these roots, there exists three waves corresponding to decreasing orders of their velocities, namely quasi-longitudinal, quasi-transverse and quasi-thermal waves. The phase velocity is given by

$V_j = \frac{\omega}{|Re(k_j)|}$, j=1,2,3

where V_j, j=1,2,3 are the phase velocities of QL, QTS and QT waves respectively.

4. Wave solution

Let a plane P or SV wave travelling through the nonlocal elastic half space $M^{(1)}$ be incident at the interface $x_3 = 0$ and makes an angle $\theta_0^{(1)}$ with the x_3 −axis.A part of this incident energy will be reflected back into the medium $M^{(1)}$ and rest will be transmitted into the medium M. Now the wave associated with transmitted energy will proceed through the medium M to interact with the boundary $x_3 = H$, where again some part of this energy will be reflected and rest will be transmitted into the medium $M^{(2)}$. The reflected energy further proceeds back to interact with the boundary $x_3 = 0$, and the process will repeat. To satisfy the boundary conditions at both the interfaces, i.e., $x_3 = 0$ and $x_3 = H$, we shall take the following reflected and refracted waves into consideration.

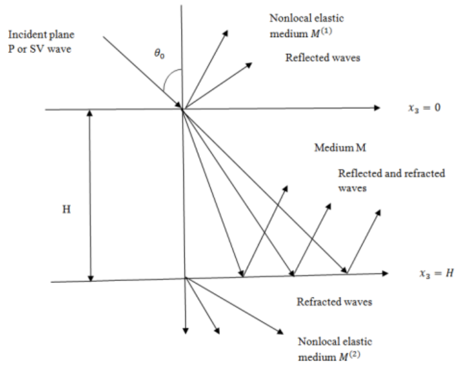

Fig. 1 Geometry of the problem

A plane longitudinal or transverse wave, making an angle θ_0 with the x_3 −axis is incident at the interface through the nonlocal elastic half space $M^{(1)}$. This wave results in

Reflected waves

(i). One reflected longitudinal wave travelling with speed $\alpha^{(1)}$ and making an angle $\theta_1^{(1)}$ with the x_3 −axis and one transverse wave propagating with speed $\beta^{(1)}$ and making an angle $\theta_2^{(1)}$ with the x_3 −axis in the medium $M^{(1)}$.

(ii) A reflected longitudinal wave, transverse wave and a thermal wave travelling with speeds v_1 , v_2 and v_3 and making angles θ_1, θ_2 and θ_3 with $x_3 -$ axis in the medium *M*.

Refracted waves

(i) A set consisting of longitudinal wave, transverse wave and a thermal wave travelling with speeds v_1 , v_2 and v_3 and making angles θ_1, θ_2 and θ_3 with x_3 −axis In the medium M.

(ii) A longitudinal wave travelling with speed $\alpha^{(2)}$ and making an angle $\theta_1^{(2)}$ with the $x_3 -$ axis and one transverse wave propagating with speed $\beta^{(2)}$ and making an angle $\theta_2^{(2)}$ with the x_3 −axis in the medium $M^{(2)}$.

We assume the wave solution for the mediums *M*, $M^{(1)}$ and $M^{(2)}$ as

Medium M

$$u_1 = \sum_{j=1}^{3}(A_j P_j^+) + \sum_{j=4}^{6}(A_j P_{j-3}^-) \tag{26}$$

$$u_3 = \sum_{j=1}^{3}(d_j A_j P_j^+) + \sum_{j=4}^{6}(d_j A_j P_{j-3}^-) \tag{27}$$

$$\varphi = \sum_{j=1}^{3}(l_j A_j P_j^+) + \sum_{j=4}^{6}(l_j A_j P_{j-3}^-). \tag{28}$$

where the coupling constants d_j and l_j are given by in Appendix B.

Medium $M^{(1)}$

$$\varphi = \sum_{j=1}^{3}(l_j A_j P_j^{+}) + \sum_{j=4}^{6}(l_j A_j P_{j-3}^{-}). \tag{28}$$

$$\phi^{(1)} = A_0^{(1)} P_0^{+(1)} + A_1^{(1)} P_0^{-(1)}, \tag{29}$$

$$\psi^{1} = B_0^{(1)} Q_1^{+(1)} + B_1^{(1)} Q_1^{-(1)} \tag{30}$$

Medium $M^{(2)}$

$$\phi^{(2)} = A_0^{(2)} P_0^{+(2)} \tag{31}$$

$$\psi^{(2)} = B_0^{(2)} Q_1^{+(2)} \tag{32}$$

Where $P_0^{+(l)} = \exp[i\omega\{(\sin\theta_0^{(l)} x_1 + cos\theta_0^{(l)} x_3)/\alpha'^{(l)} - t\}], \quad l = 1,2$

$P_0^{-(1)} = \exp[i\omega\{(\sin\theta_0^{(1)} x_1 - cos\theta_0^{(1)} x_3)/\alpha'^{(1)} - t\}]$,

$Q_1^{+(i)} = \exp[i\omega\{(\sin\theta_1^{(l)} x_1 + cos\theta_1^{(l)} x_3)/\beta'^{(l)} - t\}]$, $l = 1,2$

$Q_1^{-(1)} = \exp[i\omega\{\left(\sin\theta_1^{(1)} x_1 - cos\theta_1^{(1)} x_3\right)/\beta'^{(1)} - t\}\big]$,

$P_j^{+} = \exp\{ik_j(\sin\theta_j x_1 + cos\theta_j x_3) - i\omega t\}$,

$P_j^{-} = \exp\{ik_j(\sin\theta_j x_1 - cos\theta_j x_3) - i\omega t\}$,j=1,2,3

where $k_j = \omega/v_j$.

5. Boundary conditions

B.(1)The boundary conditions to be satisfied at the interface $x_3 = 0$ are

$$\text{(i) } t_{33} = t_{33}^{(1)}, \quad \text{(ii) } t_{31} = t_{31}^{(1)}, \quad \text{(iii) } u_1 = u_1^{(1)}, \quad \text{(iv) } u_3 = u_3^{(1)}, \text{ (v) } \frac{\partial\varphi}{\partial x_3} = 0, \tag{33}$$

B.(2) The boundary conditions to be satisfied at the interface $x_3 = H$ are

$$\text{(i) } t_{33} = t_{33}^{(2)}, \quad \text{(ii) } t_{31} = t_{31}^{(2)}, \quad \text{(iii) } u_1 = u_1^{(2)}, \quad \text{(iv) } u_3 = u_3^{(2)}, \text{ (v) } \frac{\partial\varphi}{\partial x_3} = 0. \tag{34}$$

Amplitude Ratios

Incident P wave

Using Eqs. (26)-(32) in the Eqs. (33)-(34) with the aid of (18)-(22), we obtain a non-homogeneous system of equations

$$AX=B, \tag{35}$$

where A= $[a_{ij}]_{10\times10}$, $X = [z_1, z_2, z_3, z_4, z_5, z_6, z_7, z_8, z_9, z_{10}]^t$, where 't' in the superscript represents the transpose of the matrix, $z_1 = \frac{A_1^{(1)}}{A_0^{(1)}}$, $z_2 = \frac{B_1^{(1)}}{A_0^{(1)}}$ are the reflection coefficients in the medium $M^{(1)}$, $z_i = \frac{A_i}{A_0^{(1)}}, i = 3,4,5$ are the transmission coefficients in the medium M ,$z_i = \frac{A_i}{A_0^{(1)}}$, $i = 6,7,8$ are the reflection coefficients in the medium M, $z_9 = \frac{A_0^{(2)}}{A_0^{(1)}}, z_{10} = \frac{B_0^{(2)}}{A_0^{(1)}}$ are the reflection coefficients in the medium $M^{(2)}$. Using Cramer's rule, the system of equations given in (35) enables us to amplitude ratios of various reflected and transmitted waves. The values of a_{ij} and B are given in appendix C.

Incident SV wave

In system of Eq. (35), if we replace $A_0^{(1)}$ by $B_0^{(1)}$ and equate $A_0^{(1)} = 0$, we obtain the amplitude ratios corresponding to incident SV wave.

6.Particular cases

(i) If $k_1{}^* = k_3{}^* = 0$, then from appendix C, we obtain the corresponding expressions for layered medium of two semi-infinite nonlocal elastic solids with intermediate transversely isotropic magnetothermoelastic solid without energy dissipation and with two temperature with Hall current effect and rotation.

(ii) If $a_1 = a_3 = 0$, then we obtain the expressions for layered medium of two semi-infinite nonlocal elastic solids with intermediate transversely isotropic magnetothermoelastic solid with and without energy dissipation alongwith with Hall current effect and rotation.

(iii) If we take $c_{11} = \lambda + 2\mu = c_{33}$, $c_{12} = c_{13} = \lambda$, $c_{44} = \mu$, $\beta_1 = \beta_3 = \beta$, $\alpha_1 = \alpha_3 = \alpha$, $K_1 = K_3 = K$ and $a_1 = a_3 = a$, we obtain the corresponding expressions in layered medium of two semi-infinite nonlocal elastic solids with intermediate isotropic magnetothermoelastic with two temperature and with and without energy dissipation alongwith combined effects of Hall current and rotation.

(iv) If we take $\varepsilon = 0$ we obtain the corresponding expressions for layered medium of two semi-infinite nonlocal elastic solids with intermediate transversely isotropic magnetothermoelastic solid with and without energy dissipation along with combined effects of Hall current and rotation.

7. Numerical results and discussion

For the purpose of numerical evaluation,

i) Cobalt material has been chosen for transversely isotropic magnetothermoelastic solid (medium M), following Dhaliwal and Singh(1980), as $c_{11} = 3.071 \times 10^{11} Nm^{-2}$, $c_{12} = 1.650 \times 10^{11} Nm^{-2}, c_{33} = 3.581 \times 10^{11} Nm^{-2}$, $c_{13} = 1.027 \times 10^{11} Nm^{-2}$, $c_{44} = 1.510 \times 10^{11} Nm^{-2}$, $\rho = 8.836 \times 10^{3} Kgm^{-3}$, $T_0 = 298°K$, $C_E = 4.27 \times 10^{2} JKg^{-1}deg^{-1}$, $K_1 = .690 \times 10^{2} wm^{-1}deg^{-1}$, , $K_3 = .690 \times 10^{2} wm^{-1}deg^{-1}$, $\beta_1 = 7.04 \times 10^{6} Nm^{-2}deg^{-1}$, $\beta_3 = 6.90 \times 10^{6} Nm^{-2}deg^{-1}$, $K_1^* = 0.02 \times 10^{2} Nsec^{-2}deg^{-1}$, $K_3^* = 0.04 \times 10^{2} Nsec^{-2}deg^{-1}$, $\mu_0 = 1.2571 \times 10^{-6} Hm^{-1}$, $H_0 = 1 Jm^{-1}nb^{-1}$, $\varepsilon_0 = 8.838 \times 10^{-12} Fm^{-1}$ with non-dimensional parameter L=1 and $\sigma_0 = 9.36 \times 10^{5} col^2/Cal.cm.$sec, Ω=3, $t_0 = 0.02$, M=2.5 and two temperature parameters is taken as a_1=0.03 and a_3=0.06.

ii) Copper material has been chosen for nonlocal elastic solid (medium $M^{(1)}$), following Youssef(2006) as

$\lambda = 7.76 \times 10^{10}\ Kgm^{-1}s^{-2}$, $\mu = 3.278 \times$

$10^{10}\ Kgm^{-1}s^{-2}$, $C_E = 0.6331 \times 10^3 JKg^{-1}K^{-1}$ $\rho = 8.954 \times 10^3 Kgm^{-3}$.

iii) Following Dhaliwal and Singh (1980), Magnesium material has been taken for the medium $M^{(2)}$ as

$\lambda = 2.17 \times 10^{10} Nm^2$, $\mu = 3.278 \times 10^{10} Nm^2$,$\omega_1 = 3.58 \times 10^{11} S^{-1}$, $\rho = 1.74 \times 10^3 Kgm^{-3}$, $T_0 =$ 298K , $C_E = 1.04 \times 10^3 Jkg^{-1}deg^{-1}$

Matlab software 8.4.0. has been used for numerical computation of the resulting quantities. The values of Amplitude ratios of various reflected and refracted waves, when P wave or SV wave is incident, with respect to angle of incidence θ have been computed and are depicted graphically in Figs. 2-22. A comparison has been made to show the nonlocal effect. In the Figs. 2-22.

1) The small dashed line with centre symbol circle corresponds to $\varepsilon = 0$. (local)

2) The long-dashed line with centre symbol cross corresponds $\varepsilon = 0.5$. (nonlocal)

Incident P Wave

Fig. 2 exhibits the variations of amplitude ratio Z_1 with angle of incidence θ . We notice that the variations increase in the range $5^0 \leq \theta \leq 15^0$ and then decrease sharply corresponding to both the cases and remain stationary afterwards.

Fig. 3 exhibits the variations of amplitude ratio Z_2 with angle of incidence θ. Here, we notice that corresponding to both the cases, variations are similar with a sharp jump in the values of amplitude ratio for the range $5^0 \leq \theta \leq 15^0$ followed by sharp decrease and are negligible afterwards.

Fig. 4 shows variations of amplitude ratio Z_3 with angle of incidence θ. Here, we notice that corresponding to nonlocal theory i.e., $\varepsilon = 0.5$, the variations jump sharply at $\theta = 10^0$ only and are very less otherwise. Corresponding to $\varepsilon = 0$, the variations are ascending oscillatory in the range $10^0 \leq \theta \leq 20^0$ and of very high altitude at $\theta = 25^0$ and then decrease to the bounding surface.

Fig. 5 exhibits the trends of variations of amplitude ratio Z_4 with angle of incidence θ . We notice that corresponding to $\varepsilon = 0$, initially the values of Z_4 lie on the boundary surface but as θ approaches 10^0, a sudden jump in the variations is noticed similar to Dirac delta function and when θ moves away i.e. farther from 15^0, variations with small magnitudes are noticed above the boundary surface. Corresponding to $\varepsilon = 0.5$, variations are similar with change of amplitudes.

Fig. 6 shows the trends of variations of amplitude ratio Z_5 with angle of incidence θ. We notice that initially the values are steady state for both the cases but as θ approaches 20^0, the values of amplitude ratio start varying. Corresponding to $\varepsilon = 0$, the variations are in oscillatory form whereas corresponding to $\varepsilon = 0.5$, the variations have sharp jumps in between.

Fig. 7 displays the variations of amplitude ratio Z_6 with angle of incidence θ.Here corresponding to $\varepsilon = 0$, in the initial range, there are sharp jumps whereas the pattern is oscillatory afterwards whereas corresponding to $\varepsilon = 0.5$, initially the variations are ascending oscillatory in the range $\theta \leq 20^0$, then there is a sharp jump and are very less afterwards.

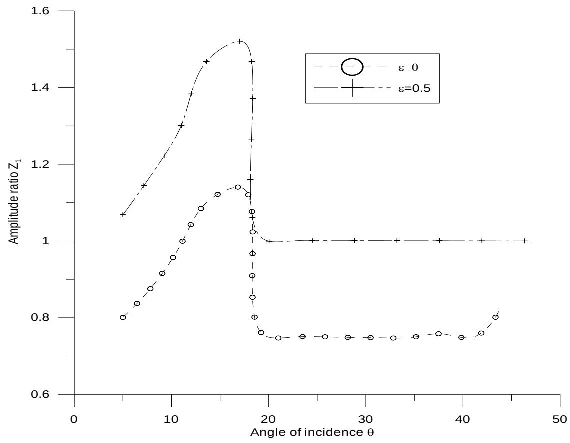

Fig. 2 Variations of Amplitude ratio Z_1 with angle of incidence θ (Incident P wave)

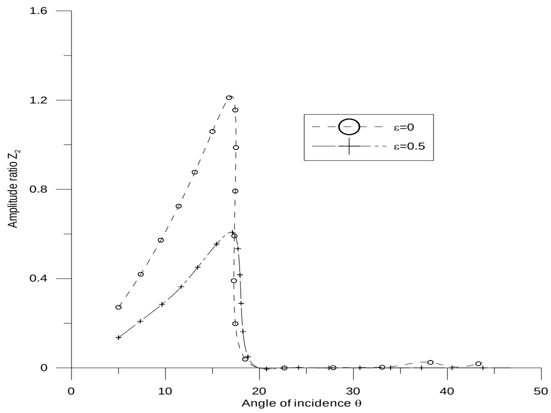

Fig. 3 Variations of Amplitude ratio Z_2 with angle of incidence θ (Incident P wave)

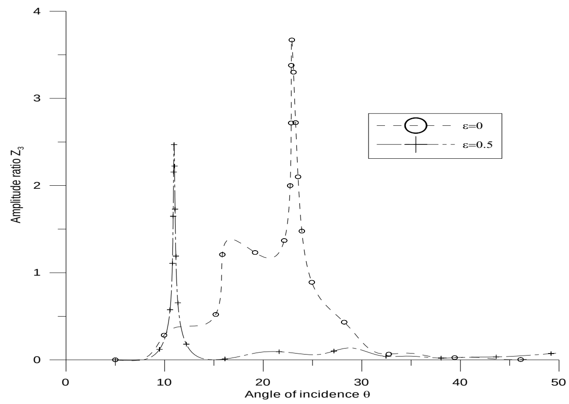

Fig. 4 Variations of Amplitude ratio Z_3 with angle of incidence θ (Incident P wave)

Fig. 8 displays the variations of amplitude ratio Z_7 with angle of incidence θ.It is noticed that corresponding to $\varepsilon = 0$, the variations are in form of Dirac delta function for the range $10^0 \leq \theta \leq 15^0$ and are oscillatory afterwards. Corresponding to $\varepsilon = 0.5$, the variations are similar with a difference in range.

Fig. 9 displays the variations of amplitude ratio Z_8 with angle of incidence θ.Corresponding to $\varepsilon = 0$, in the range $5^0 \leq \theta \leq 10^0$, the variations show a sharp jump and are ascending oscillatory afterwards in the rest. Corresponding

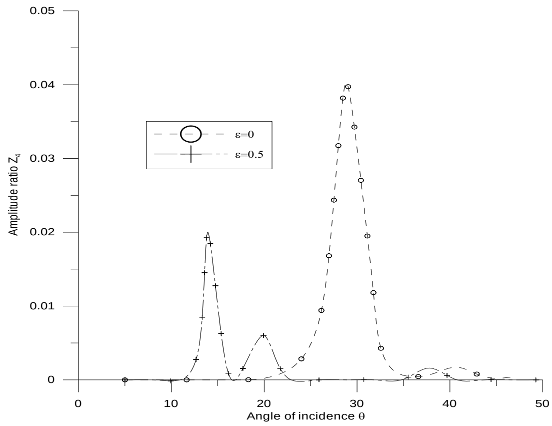

Fig. 5 Variations of Amplitude ratio Z_4 with angle of incidence θ (Incident P wave)

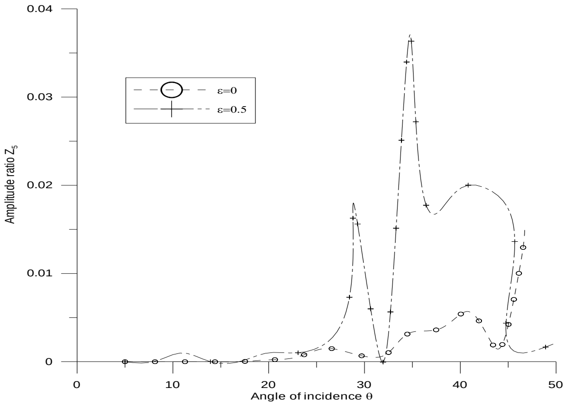

Fig. 6 Variations of Amplitude ratio Z_5 with angle of incidence θ (Incident P wave)

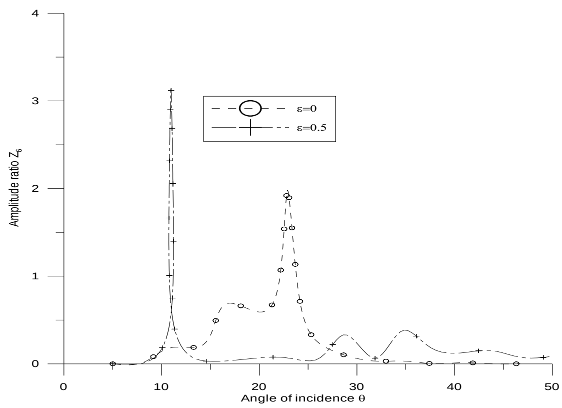

Fig. 7 Variations of Amplitude ratio Z_6 with angle of incidence θ (Incident P wave)

to $\varepsilon = 0.5$, the variations are in oscillatory form in the range $5^0 \leq \theta \leq 25^0$, followed by sharp jumps in the rest. Fig. 10 exhibits the variations of amplitude ratio Z_9 with angle of incidence θ .Corresponding to $\varepsilon = 0$, the variations are descending oscillatory whereas corresponding to $\varepsilon = 0.5$, in the intial range there is a sharp jump in the variations and are negligible afterwards.

Fig. 11 displays the variations of amplitude ratio Z_{10} with angle of incidence θ. Corresponding to both the cases, initially the value of amplitude ratio is very high followed

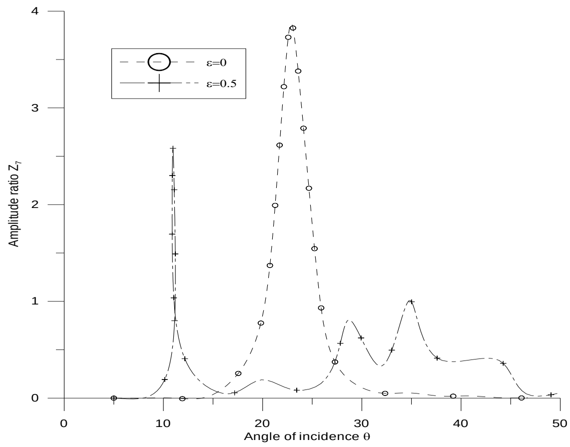

Fig. 8 Variations of Amplitude ratio Z_7 with angle of incidence θ (Incident P wave)

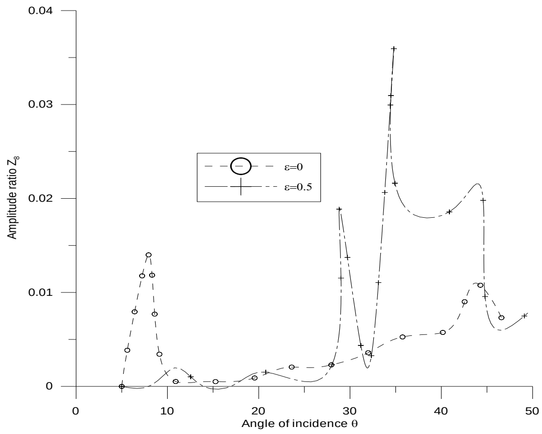

Fig. 9 Variations of Amplitude ratio Z_8 with angle of incidence θ (Incident P wave)

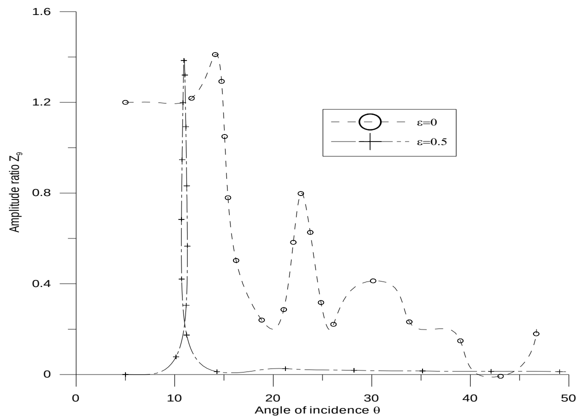

Fig. 10 Variations of Amplitude ratio Z_9 with angle of incidence θ (Incident P wave)

by a sharp decrease and small in the rest.

Incident SV Wave

Fig. 12, exhibits the variations of amplitude ratio Z_1 with angle of incidence θ.Here corresponding to $\varepsilon = 0$, the variations are oscillatory in the range $5^0 \leq \theta \leq 25^0$ and then increase in the range $25^0 \leq \theta \leq 45^0$ followed by a decrease in the rest. Corresponding to $\varepsilon = 0.5$, the variations are similar to $\varepsilon = 0$ in the range $5^0 \leq \theta \leq 45^0$

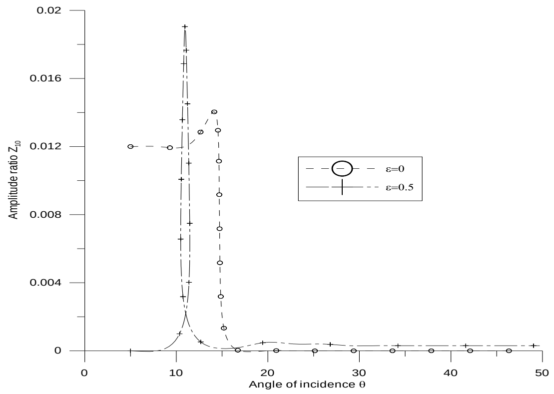

Fig. 11 Variations of Amplitude ratio Z_{10} with angle of incidence θ (Incident P wave)

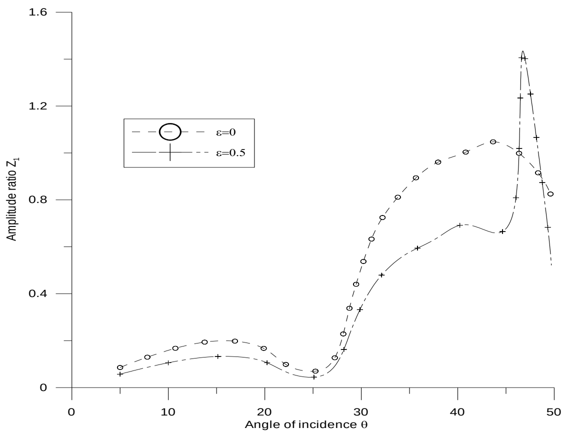

Fig. 12 Variations of Amplitude ratio Z_1 with angle of incidence θ (Incident SV wave)

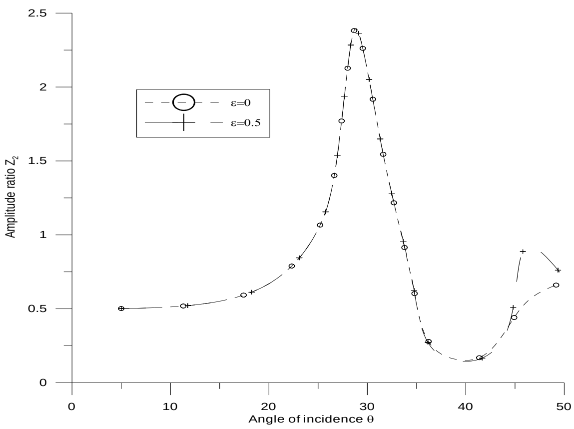

Fig. 13 Variations of Amplitude ratio Z_2 with angle of incidence θ (Incident SV wave)

whereas a sharp jump is seen afterwards.

Fig. 13 exhibits the variations of amplitude ratio Z_2 with angle of incidence θ. Here, corresponding to both the cases, variations are similar with an increase in the range $5^0 \leq \theta \leq 30^0$, decrease in the range $35^0 \leq \theta \leq 40^0$ and increase in the rest.

Fig. 14 shows the trends of variations of amplitude ratio Z_3 with angle of incidence θ.Here, we notice that corresponding $\varepsilon = 0$, the variations are in ascending oscillatory pattern in the whole range whereas

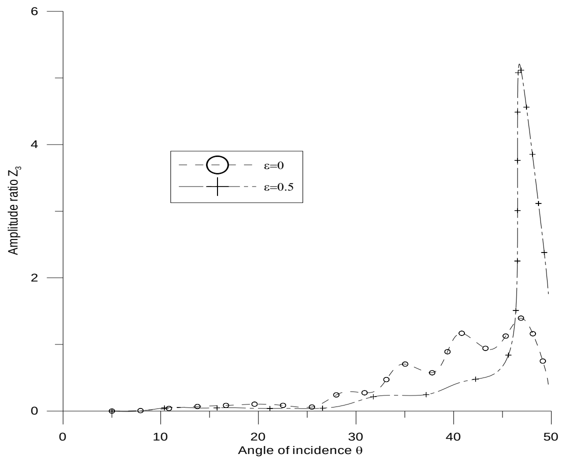

Fig. 14 Variations of Amplitude ratio Z_3 with angle of incidence θ (Incident SV wave)

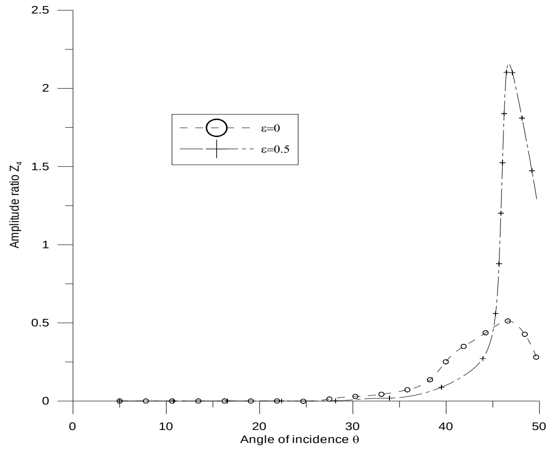

Fig. 15 Variations of Amplitude ratio Z_4 with angle of incidence θ (Incident SV wave)

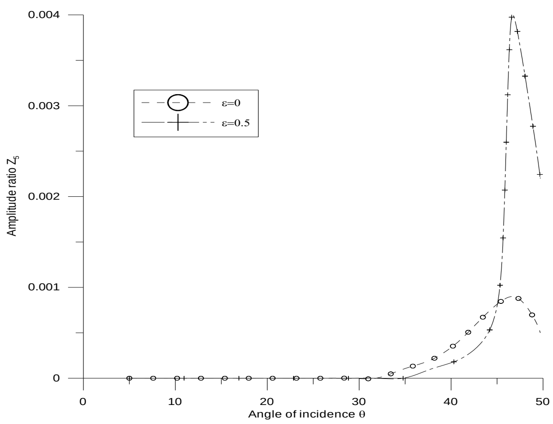

Fig. 16 Variations of Amplitude ratio Z_5 with angle of incidence θ (Incident SV wave)

corresponding to $\varepsilon = 0.5$, the variations are oscillatory in the range $5^0 \leq \theta \leq 45^0$ followed by a sharp jump.

Fig. 15 exhibits the trends of variations of amplitude ratio Z_4 with angle of incidence θ. We notice that corresponding to both the cases, initially the values of Z_4 lie on the boundary surface but as θ approaches 30^0, the

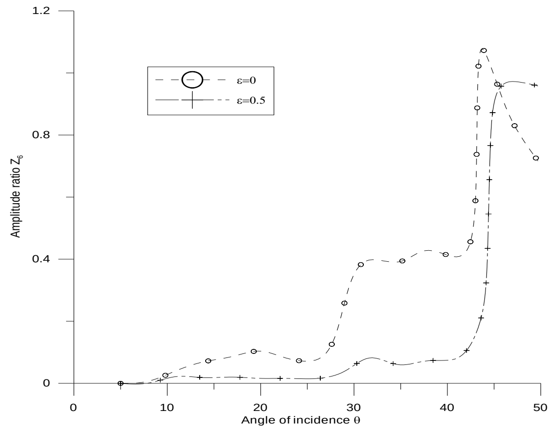

Fig. 17 Variations of Amplitude ratio Z_6 with angle of incidence θ (Incident SV wave)

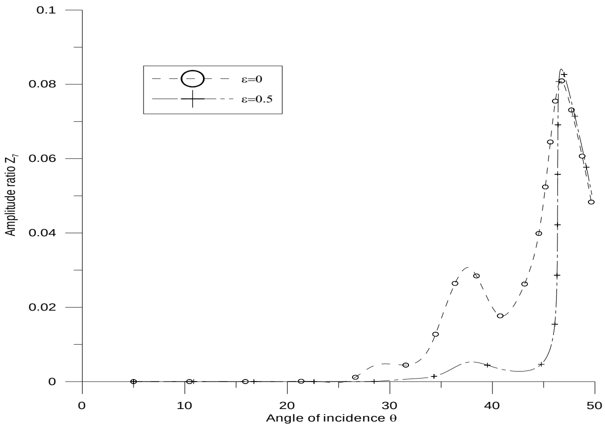

Fig. 18 Variations of Amplitude ratio Z_7 with angle of incidence θ (Incident SV wave)

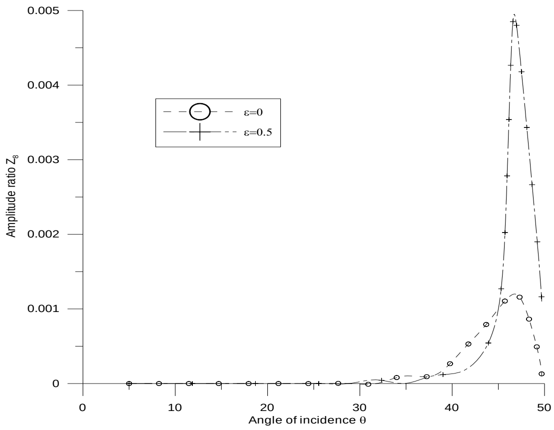

Fig. 19 Variations of Amplitude ratio Z_8 with angle of incidence θ (Incident SV wave)

variations are noticed. corresponding to $\varepsilon = 0$, the trend is oscillatory in the range $35^0 \leq \theta \leq 50^0$. Corresponding to $\varepsilon = 0.5$, a sharp increase is seen in the range $35^0 \leq \theta \leq 45^0$ with a sharp decrease in the rest.

Fig. 16 exhibits the trends of variations of amplitude ratio Z_5 with angle of incidence θ. Here the similar variations are noticed as in Fig. 15.

Fig. 17 displays the variations of amplitude ratio Z_6 with angle of incidence θ. Here corresponding to both the

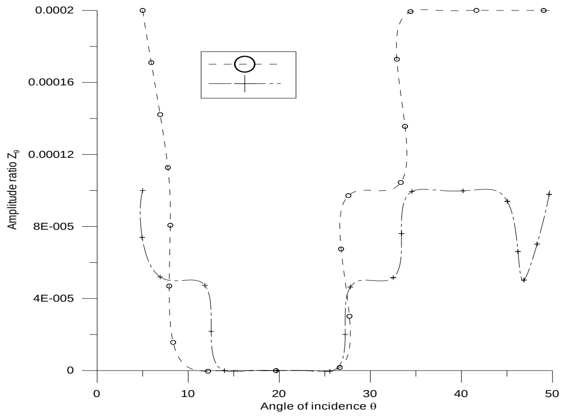

Fig. 20 Variations of Amplitude ratio Z_9 with angle of incidence θ (Incident SV wave)

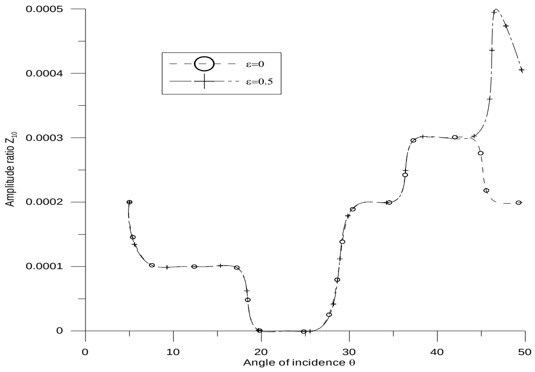

Fig. 21 Variations of Amplitude ratio Z_{10} with angle of incidence θ (Incident SV wave)

cases, the variations in amplitude ratio move away from the boundary surface in form of ascending pattern of waves as θ increases.

Fig. 18 displays the variations of amplitude ratio Z_7 with angle of incidence θ. It is noticed that corresponding to both the cases, the variations are in oscillatory form with different amplitudes.

Fig. 19 displays the variations of amplitude ratio Z_8 with angle of incidence θ. Here similar trends are noticed as in Fig. 18 with change in magnitude.

Fig. 20 exhibits the variations of amplitude ratio Z_9 with angle of incidence θ. Corresponding to $\varepsilon = 0$, initially a sharp decrease is seen and the values of amplitude ratio remain stationary for the range $10^0 \leq \theta \leq 25^0$, and as θ approaches 25^0, increase in form of step is noticed up to $\theta = 35^0$ and the values remain stationary upto $\theta = 50^0$. Corresponding to $\varepsilon = 0.5$, the variations are similar with change in the range and amplitude.

Fig. 21 displays the variations of amplitude ratio Z_{10} with angle of incidence θ. Here similar variations are noticed as discussed in Fig. 20.

8. Conclusions

Important phenomena are noticed in all the graphical representations of amplitude ratios. These phenomena permit us some concluding remarks.

1. The variations follow sharp increase and decrease in form of seismic waves. In the absence of nonlocal parameter, the variations follow oscillatory pattern whereas in the presence of nonlocal parameter less oscillations are observed.

2. Effect of nonlocal parameter is quite evident from the trends of variations corresponding to both the cases i.e. presence and absence of nonlocal parameter.

3. When P wave is incident, we notice that the variations approach the boundary surface as we move away from the source.

4. When SV wave is incident, the variations move away from the boundary surface as we move away from the source.

5. Variations in all the amplitude ratios corresponding to both the case are very small near boundary surface in the initial range.

6. These trends obey elastic and thermoelastic properties of a solid under investigation and all the results are in agreement with the thermoelasticity theory.

7. The layered structure considered here can be widely used in diverse applications such as spacecraft, aircraft, automobiles, boats and ships due to their substantial bending strength.

8. The present theoretical results may provide interesting information for experimental scientists/researchers/ seismologists working on this subject. The used methods in the present article is applicable to a wide range of problems in thermodynamics and thermoelasticity.

9. References

Achenbach, J.D. (1973), *Wave Propagation in Elastic Solids*, Elsevier, North-Holland, Amsterdam.

Atwa, S.Y. and Jahangir, A. (2014), "Two temperature effects on plane waves in generalized thermo-microstretch elastic solid", *J. Thermophys*., **35**(1), 175-193.

Boley, B.A. and Tolins, I.S. (1962), "Transient coupled thermoelastic boundary value problem in the half space", *J. Appl. Mech*., **29**(4), 637-646.

Chandrasekharaiah, D.S. (1998), "Hyperbolic thermoelasticity: A review of recent literature", *Appl. Mech. Rev*., **51**(12), 705-729.

Chaudhary, S., Kaushik, V.P. and Tomar, S.K. (2010), "Transmission of plane SH-waves through a monoclinic layer embedded between two different self-reinforced elastic solid half-spaces", *J. Appl. Math. Mech*., **6**(19), 22-43.

Chen, P.J. and Gurtin, M.E. (1968), "On a theory of heat conduction involving two parameters", *Zeitschrift für Angewandte Mathematik und Physik (ZAMP)*, **19**, 614-627.

Chen, P.J., Gurtin, M.E. and Williams, W.O. (1968), "A note on simple heat conduction", *J. Appl. Math. Phys. (ZAMP)*, **19**, 969-970.

Chen, P.J., Gurtin, M.E. and Williams, W.O. (1969), "On the thermodynamics of non-simple elastic materials with two temperatures", *J. Appl. Math. Phys. (ZAMP)*, **20**(1), 107-112.

Das, P. and Kanoria, M. (2014), "Study of finite thermal waves in a magnetothermoelastic rotating medium", *J. Therm. Stress*., **37**(4), 405-428.

Deshpande, V.S. and Fleck, N.A. (2005), "One-dimensional response of sandwich plates to underwater shock loading", *J. Mech. Phys. Sol*., **53**(11), 2347-2383.

Dhaliwal, R.S. and Singh, A. (1980), *Dynamic Coupled Thermoelasticity*, Hindustance Publisher Corp., New Delhi, India.

Edelen, D.G.B. and Laws, N. (1971), "On the thermodynamics of systems with non-locality", *Arch. Rat. Mech. Analy*., **43**(1), 36-44.

Elphinstone, M.J. and Lakhtakia, A. (1994), "Plane wave response of an elastic chiral solid slab sandwiched between achiral solid half spaces", *J. Acoust. Soc. Am*., **95**(2), 617-627.

Eringen, A.C. (1972), "Nonlocal polar elastic continua", *J. Eng. Sci*., **10**(1), 1-16.

Eringen, A.C. and Edelen, D.G.B. (1972), "On nonlocal elasticity", *J. Eng. Sci*., **10**(3), 233-248.

Ezzat, M.A. and AI-Bary, A.A. (2017), "Fractional magneto-thermoelastic materials with phase lag green-naghdi theories", *Steel Compos. Struct*., **24**(3), 297-307.

Ezzat, M.A., EI-Karamany, A.S. and EI-Bary, A.A. (2016), "Modelling of memory dependent derivative in generalized thermoelasticity", *Eur. Phys. J. Plus*, **131**(10), 372.

Green, A.E. and Naghdi, P.M. (1991), "A re-examination of the basic postulates of thermomechanics", *Proceedings of the Royal Society of London Series A*, **432**(1885), 171-194.

Green, A.E. and Naghdi, P.M. (1992), "On undamped heat waves in an elastic solid", *J. Therm. Stress*., **15**(2), 253-264.

Green, A.E. and Naghdi, P.M. (1993), "Thermoelasticity without energy dissipation", *J. Elast*., **31**(3), 189-208.

Jahangir, A. (2012), "Propagation of plane magneto-thermo-elastic waves in a rotating, electrically conducting and transversely isotropic medium", *Sci. Res. Essays*, **7**(10), 1148-1155.

Kaushal, S., Kumar, R. and Miglani, A. (2011), "Wave propagation in temperature rate dependent thermoelasticity with two temperatures", *Math. Sci*., **5**, 125-146.

Keith, C.M. and Crampin. (1977), "Seismic body waves in anisotropic media, reflection and refraction at a plane interface", *Geophys. J. Int*., **49**(1), 181-208.

Khurana, A. and Tomar, S.K. (2009), "Longitudinal wave response of a chiral slab interposed between micropolar half-spaces", *J. Sol. Struct*., **46**(1), 135-150.

Kroner, E. (1967), "Elasticity theory of materials with long range cohesive forces", *J. Sol. Struct*., **3**(5), 731-742.

Kumar, R., Sharma, N. and Lata, P. (2017), "Effects of hall current and two temperatures in transversely isotropic magnetothermoelastic with and without energy dissipation due to ramp type heat", *Mech. Adv. Mater. Struct*., **24**(8), 625-635.

Kumar, R., Sharma, N. and Lata, P. (2016b), "Thermomechanical interactions due to hall current in transversely isotropic thermoelastic with and without energy dissipation with two temperature and rotation", *J. Sol. Mech*., **8**(4), 840-858.

Kumar, R. and Gupta, V. (2013), "Plane wave propagation in an anisotropic thermoelastic medium with fractional order derivative and void", *J. Thermoelast*., **1**(1), 21-34.

Kumar, R., Sharma, N. and Lata, P. (2016a), "Thermomechanical interactions in transversely isotropic magneto thermoelastic medium with vacuum and with and without energy dissipation with combined effects of rotation, vacuum and two temperature", *Appl. Math. Model*., **40**(13-14), 6560-6575.

Kumar, R., Sharma, N. and Lata, P. (2016), "Effects of hall current in a transversely isotropic magnetothermoelastic with and without energy dissipation due to normal force", *Struct. Eng. Mech*., **57**(1), 91-103.

Kumar, R. and Mukhopdhyay, S. (2010), "Effects of thermal relaxation times on plane wave propagation under two temperature thermoelasticity", *J. Eng. Sci*., **48**(2), 128-139.

Kumar, R. and Kansal, T. (2011), "Reflection of plane waves at the free surface of a transversely isotropic thermoelastic diffusive solid half-space", *J. Appl. Math. Mech*., **7**(14), 57-78.

Lata, P., Kumar, R. and Sharma, N. (2016), "Plane waves in

anisotropic thermoelastic medium", *Steel Compos. Struct.*, **22**(3), 567-587.
Liu, L. and Bhattacharya, K. (2009), "Wave propagation in a sandwich structure", *J. Sol. Struct.*, **46**(17), 3290-3300.
Marin, M. and Baleanu, D. (2016), "On vibrations in thermoelasticity without energy dissipation for micropolar bodies", *Bound. Val. Prob.*, 1-19.
Marin, M. (1997), "On weak solutions in elasticity of dipolar bodies with voids", *J. Comput. Appl. Math.*, **82**(1-2), 291-297.
Marin, M. (2008), "Weak solutions in elasticity of dipolar porous materials", *Math. Prob. Eng.*, 1-8.
Marin, M. (2016), "An approach of a heat flux dependent theory for micropolar porous media", *Meccan.*, **51**(5), 1127-1133.
Othman, M.I.A. and Abd-Elaziz, E.M. (2017), "Plane waves in a magneto-thermoelastic solids with voids and microtemperatures due to hall current and rotation", *Result. Phys.*, **7**, 4253-4263.
Othman, M.I.A. and Jahangir, A. (2015), "Plane waves on rotating microstretch elastic solid with temperature dependent elastic properties", *Appl. Math. Informat. Sci.*, **9**(6), 2963-2972.
Othman, M.I.A. (2010), "Generalized electro-magneto-thermoelasticity in case of thermal shock waves for a finite conducting half-space with two relaxation times", *Mech. Mech. Eng.*, **14**(1), 5-30.
Polizzotto, C. (2001), "Nonlocal elasticity and related variational principles", *J. Sol. Struct.*, **38**, 7359-7380.
Said, M.S. and Othman, M.I.A. (2016), "Wave propagation in a two temperature fibre-reinforced magneto-thermoelastic medium with three phase lag models", *Struct. Eng. Mech.*, **57**(2), 201-220.
Sharma, K. and Marin, M. (2013), "Effect of distinct conductive and thermodynamic temperatures on the reflection of plane waves in micropolar elastic half-space", *Univ. Politeh. Bucharest Sci. Bullet. Ser.*, **75**(2), 121-132.
Sharma, K. and Bhargava, R.R. (2014), "Propagation of thermoelastic plane waves at an imperfect boundary of thermal conducting viscous liquid/generalized thermolastic solid", *Afrika Mathematika*, **25**, 81-102.
Singh, D., Kaur, G. and Tomar, S.K. (2017), "Waves in nonlocal elastic solids with voids", *J. Elast.*
Slaughter, W.S. (2002), *The Linearised Theory of Elasticity*, Birkhausar.
Vasiliew, V.V. and Lurie, S.A. (2016), "On correct nonlocal generalized theories of elasticity", *Phys. Mesomech.*, **19**(3), 269-281.
Warren, W.E. and Chen, P.J. (1973), "Wave propagation in the two temperature theory of thermoelasticity", *J. Acta Mech.*, **16**, 21-33.
Youssef, H.M. (2006), "Theory of two temperature generalized thermoelasticity", *IMA J. Appl. Math.*, **71**(3), 383-390.
Youssef, H.M. (2011), "Theory of two-temperature thermoelasticity without energy dissipation", *J. Therm. Stress.*, **34**(2), 138-146.

CC

Appendix A

Where

$$A = \zeta_4\zeta_5\zeta_6 - cos^2\theta\,\zeta_2\zeta_7 p_1 - \delta_1\zeta_8^2\zeta_1\zeta_4 + \zeta_2\zeta_7\zeta_8 + \zeta_2\zeta_7\zeta_8^2\zeta_1$$

$$B = -\zeta_1\zeta_4\zeta_6 - \zeta_1 cos^2\theta\,\zeta_2\zeta_7 p_1 + \omega^2\zeta_6\zeta_5 - \zeta_4\zeta_5\zeta_1 + \zeta_5 cos^2\theta\,\zeta_7 p_1 - \delta_1\zeta_4\zeta_3\zeta_8 + \zeta_2\zeta_7\zeta_8 - \delta_1\omega^2\zeta_1\zeta_8^2 + \zeta_3\zeta_8\zeta_1\zeta_4 - \zeta 1_8^2\zeta_1\zeta_7 - \zeta_2\zeta_8\zeta_3\zeta_7 + \delta_1\zeta_8\zeta_7 + p_1\zeta_7\zeta_6 sin^2\theta - sin^2\theta\,\zeta_2\zeta_7 p_1$$

$$C = -\zeta_5\zeta_1\omega^2 - \zeta_1\zeta_6\omega^2 + \zeta_1^2\zeta_4 - \zeta_1 cos^2\theta\,\zeta_7 p_1 - \zeta_3\delta_1\omega^2\zeta_8 + \zeta_3^2\zeta_4 + \zeta_8\zeta_3\zeta_1\omega^2 - \zeta_1\,\varepsilon_5{}'\beta_1^2\omega^2 sin^2\theta$$

$$D = \omega^2(\zeta_1^2 - \zeta_3^2)$$

$\zeta_1 = \left(\frac{\varepsilon_0\mu_0^2 H_0^2}{\rho} + 1\right)\omega^2 + \Omega^2$, $\zeta_2 = \frac{a_1}{L}sin^2\theta + \frac{a_3}{L}cos^2\theta$, $\zeta_3 = -2i\omega\Omega$, $\zeta_4 = \zeta_2\omega^2 - sin^2\theta(\varepsilon_1 + i\varepsilon_3) - cos^2\theta\,(\varepsilon_2 + i\varepsilon_4)$, $\zeta_5 = sin^2\theta + \delta_2 cos^2\theta$, $\zeta_6 = \delta_2 sin^2\theta + \delta_3 cos^2\theta$, $\zeta_7 = \varepsilon_5{}'\omega^2\beta_1\beta_3$, $\zeta_8 = -sin\theta cos\theta$, $p_5 = \frac{\beta_3}{\beta_1}$

Appendix B

$$d_j = [k_j^4\{\eta_j(\delta_1 sin^2\theta_j\varepsilon_{13} + \delta_1 cos^2\theta_j\varepsilon_{24} - \delta_1\zeta_j + \varepsilon_5'\beta_1\beta_3\omega^2\zeta_j\} + k_j^2\{-\delta_1\omega^2\eta_j + (M_0 + 2\Omega)i\omega(\varepsilon_{13}sin^2\theta_j + cos^2\theta_j\varepsilon_{24}\} - \omega^2(M_0 + 2\Omega)i\omega\,]/D\ , \quad j = 1,2,3$$

$$l_j = [k_j^3\{-\delta_1\eta_j\varepsilon_5'\beta_1\beta_3\omega^2 i cos\theta_j + (\delta_2 i sin^3\theta_j + \delta_3 i cos^2\theta_j sin\theta_j)\varepsilon_5'\beta_1^2\omega^2\} + ik_j\{(M_0 i\omega + 2i\omega\Omega)\left(\varepsilon_5'\beta_1\beta_3\omega^2 cos\theta_j\right) + \left(\frac{M_0}{m}i\omega + \omega^2 + \Omega^2\right)(\varepsilon_5' sin\theta_j\beta_1^2\omega^2)\}]/D\ , \ j = 1,2,3$$

$$D = k_j^4\left(\varepsilon_{13}\delta_2 sin^4\theta_j + \varepsilon_{13}\delta_3\eta_j^2 + \delta_2\varepsilon_{24}\eta_j^2 + \varepsilon_{24}\delta_3 cos^4\theta_j - \delta_2\omega^2 sin^2\theta_j\zeta_j - \omega^2\delta_3 cos^2\theta_j\eta_j - \beta_3^2\varepsilon_5'\omega^2 cos^2\theta_j\eta_j\right) + k_j^2\left\{\left(-sin^2\theta_j\delta_2 - \delta_3 cos^2\theta_j\right)\omega^2 + \left(\frac{M_0}{m}i\omega + \omega^2 + \Omega^2\right)\left(-\varepsilon_{13}sin^2\theta_j - \varepsilon_{24}cos^2\theta_j + \omega^2\zeta_j\right) - \beta_3^2\varepsilon_5'\omega^2 cos^2\theta_j\right\} + \left(\frac{M_0}{m}i\omega + \omega^2 + \Omega^2\right)\omega^2\ ,\ j = 1,2,3$$

$$d_j = [k_j^4\{\eta_j(\delta_1 sin^2\theta_j\varepsilon_{13} + \delta_1 cos^2\theta_j\varepsilon_{24} + \delta_1\zeta_j - \varepsilon_5'\beta_1\beta_3\omega^2\zeta_j\} + k_j^2\{-\delta_1\omega^2\eta_j + (M_0 + 2\Omega)i\omega(\varepsilon_{13}sin^2\theta_j + cos^2\theta_j\varepsilon_{24}\} - \omega^2(M_0 + 2\Omega)i\omega\,]/D\ , \quad j = 4,5,6$$

$$l_j = [k_j^3\{\delta_1\eta_j\varepsilon_5'\beta_1\beta_3\omega^2 i cos\theta_j + (\delta_2 i sin^3\theta_j + \delta_3 i cos^2\theta_j sin\theta_j)\varepsilon_5'\beta_1^2\omega^2\} + ik_j\{(M_0 i\omega + 2i\omega\Omega)\left(\varepsilon_5'\beta_1\beta_3\omega^2 cos\theta_j\right) + \left(\frac{M_0}{m}i\omega + \omega^2 + \Omega^2\right)(\varepsilon_5' sin\theta_j\beta_1^2\omega^2)\}]/D\ \ j = 4,5,6$$

$$\eta_j = sin\theta_j cos\theta_j\ ,\ \varepsilon_{13} = \varepsilon_1 - i\varepsilon_3\omega,\ \varepsilon_{24} = \varepsilon_2 - i\varepsilon_4\omega,$$

$$\zeta_j = \frac{a_1}{L}sin^2\theta_j + \frac{a_3}{L}cos^2\theta_j\ ,$$

$$M_0 = \frac{M}{1 + m^2}\,\mu_0 H_0 m$$

Appendix C

$a_{11} = i\sin\theta$, $a_{12} = i/\beta'^{(1)}\sqrt{\omega^2 - {\beta'^{(1)}}^2 sin^2\theta}$, $a_{13} = -1$, $a_{14} = -1$, $a_{15} = -1$, $a_{16} = -1$, $a_{17} = -1$, $a_{18} = -1$,

$a_{19}=0,\ a_{1,10}=0, a_{21}=-i/\alpha'^{(1)}\sqrt{\omega^2-\alpha'^{(1)^2}(sin^2\theta)},$ $a_{22}=isin\theta,\ a_{23}=-d_1,\ a_{24}=-d_2, a_{25}=-d_3, a_{26}=-d_4, a_{27}=-d_5, a_{28}=-d_6,\ a_{29}=0\ ,\ a_{2,10}=0\ , a_{31}=(\omega^2-\alpha'^{(1)^2})(sin\theta)^2-\frac{\alpha'^{(1)^2}\gamma'^{(1)^2}}{\omega^2}(sin\theta)^2,\ a_{32}=\frac{(\alpha'^{(1)^2}-\gamma'^{(1)^2})}{\beta'^{(1)}}sin\theta\sqrt{\omega^2-\beta'^{(1)^2}sin^2\theta}$

$a_{3j}=-\Delta_j,\ j=3,4,5$ where $\Delta_j=\frac{c_{11}}{\rho c_1^2}i\ sin\theta+\frac{c_{13}}{\rho c_1^2}i\frac{d_j}{v_j}\sqrt{\omega^2-v_j{}^2(sin\theta)^2}-\frac{\beta_3}{\beta_1}l_j\left(1-\frac{v_j{}^2}{\omega^2}sin^2\theta\frac{a_1}{L}\right)-\frac{\beta_3}{\beta_1}\frac{a_3l_j\omega}{Lv_j{}^2}\sqrt{\omega^2-v_j{}^2(sin\theta)^2}$, $a_{3j}=-\Delta'_j,\ j=6,7,8$, where $\Delta'_j=\frac{c_{11}}{\rho c_1^2}i\ sin\theta-\frac{c_{13}}{\rho c_1^2}i\frac{d_j}{v_j}\sqrt{\omega^2-v_j{}^2(sin\theta)^2}-\frac{\beta_3}{\beta_1}l_j\left(1-\frac{v_j{}^2}{\omega^2}sin^2\theta\frac{a_1}{L}\right)-\frac{\beta_3}{\beta_1}\frac{a_3l_j\omega}{Lv_j{}^2}\sqrt{\omega^2-v_j{}^2(sin\theta)^2},\ a_{39}=0,$ $a_{3,10}=0, a_{41}=\frac{\beta'^{(1)^2}}{\alpha'^{(1)}}\sqrt{\omega^2-\alpha'^{(1)^2}(sin\theta)^2}$, $a_{42}=\omega^2-v_1{}^2(sin\theta)^2,\ a_{4j}=-\eta_j, j=3,4,5,6,7,8$ where $\eta_j=\frac{c_{44}}{\rho c_1^2}\left(\frac{-i\sqrt{\omega^2-v_j{}^2(sin\theta)^2}}{v_j}+\frac{d_ji\omega}{v_j}sin\theta\right), j=3,4,5$ and $\eta_j=\frac{c_{44}}{\rho c_1^2 S}\left(\frac{i\sqrt{\omega^2-v_j{}^2(sin\theta)^2}}{v_j}+\frac{d_ji\omega}{v_j}sin\theta\right), j=6,7,8,\ a_{49}=0, a_{4,10}=0,\ a_{5j}=0, j=1,2,9,10.\ a_{5j}=\frac{l_j}{v_j}\sqrt{\omega^2-v_j{}^2(sin\theta)^2},\ j=3,4,5, a_{5j}=-\frac{l_j}{v_j}\sqrt{\omega^2-v_j{}^2(sin\theta)^2},\ j=6,7,8.,$

$a_{6j}=0, j=1,2.\ a_{69}=isin\theta,\ a_{6,10}=-i/\beta'^{(2)}(\sqrt{\omega^2-\beta'^{(2)^2}(sin^2\theta)}, a_{6j}=-1, j=3,4,5,6,7,8., a_{7j}=0, j=1,2, a_{7j}=-d_j,\ j=3,4,5,6,7,8.,$ $a_{79}=i\omega/\alpha'^{(2)^2}\sqrt{\omega^2-\alpha'^{(2)^2}(sin\theta)^2}$, $a_{7,10}=isin\theta,$ $a_{8j}=0,\ j=1,2,\ a_{8j}=-\Delta_j,\ j=3,4,5$ where $\Delta_j=\frac{c_{11}}{\rho c_1^2}i\ sin\theta+\frac{c_{13}}{\rho c_1^2}i\frac{d_j}{v_j}\sqrt{\omega^2-v_j{}^2(sin\theta)^2}-\frac{\beta_3}{\beta_1}l_j\left(1-\frac{v_j{}^2}{\omega^2}sin^2\theta\frac{a_1}{L}\right)-\frac{\beta_3}{\beta_1}\frac{a_3l_j\omega}{Lv_j{}^2}\sqrt{\omega^2-v_j{}^2(sin\theta)^2}$, $a_{8j}=-\Delta'_j,$ $j=6,7,8$, where $\Delta'_j=\frac{c_{11}}{\rho c_1^2}i\ sin\theta-\frac{c_{13}}{\rho c_1^2}i\frac{d_j}{v_j}\sqrt{\omega^2-v_j{}^2(sin\theta)^2}-\frac{\beta_3}{\beta_1}l_j\left(1-\frac{v_j{}^2}{\omega^2}sin^2\theta\frac{a_1}{L}\right)-\frac{\beta_3}{\beta_1}\frac{a_3l_j\omega}{Lv_j{}^2}\sqrt{\omega^2-v_j{}^2(sin\theta)^2},\ a_{89}=-\gamma'^{(2)^2}sin^2\theta-(\omega^2-\alpha'^{(2)^2}sin^2\theta),\ a_{8,10}=\frac{sin\theta}{\beta'^{(2)}}\sqrt{\omega^2-\beta'^{(2)^2}sin^2\theta}\ (\gamma'^{(2)}+\frac{\alpha'^{(2)^2}}{\omega^2}),\ a_{9j}=0\ ,\ j=1,2,\ a_{4j}=-\eta_j, j=3,4,5,6,7,8$

where $\eta_j=\frac{c_{44}}{\rho c_1^2}\left(\frac{-i\sqrt{\omega^2-v_j{}^2(sin\theta)^2}}{v_j}+\frac{d_ji\omega}{v_j}sin\theta\right), j=3,4,5$

and $\eta_j=\frac{c_{44}}{\rho c_1^2}\left(\frac{i\sqrt{\omega^2-v_j{}^2(sin\theta)^2}}{v_j}+\frac{d_ji\omega}{v_j}sin\theta\right), j=6,7,8,$

$a_{99}=\frac{sin\theta}{\alpha'^{(2)}}\sqrt{\omega^2-\alpha'^{(2)^2}sin^2\theta}$, , $a_{9,10}=sin^2\theta+\frac{\omega^2-\beta'^{(2)^2}(sin^2\theta)}{\omega^2}$, $a_{10,j}=0,\ j=1,2,9,10.\ a_{10,j}=\frac{l_j}{v_j}\sqrt{\omega^2-v_j{}^2(sin\theta)^2},\ j=3,4,5, a_{10,j}=-\frac{l_j}{v_j}\sqrt{\omega^2-v_j{}^2(sin\theta)^2},\ j=6,7,8.,$

$d_1=-a_{11},\ d_2=a_{21},\ d_3=-a_{31},\ d_4=a_{41},\ d_j=0, j=5,6,7,8,9,10$

For incident SV wave

$d_1=-a_{12},\ d_2=-a_{22},\ d_3=-a_{32},\ d_4=-a_{42},\ d_j=0, j=5,6,7,8,9,10$